Sample Preconcentration in Nanochannels with Nonuniform Surface Charge and Thick Electric Double Layers

A. Eden[*1], C. McCallum[1], B. Storey[2], S. Pennathur[1], C. D. Meinhart[1]
[1]University of California, Santa Barbara, [2]Olin College
*Corresponding author: Department of Mechanical Engineering, University of California, Santa Barbara, Santa Barbara, CA 93106-5070. Email: a_eden@engineering.ucsb.edu

Abstract: We present a novel method for concentrating and focusing small analytes by taking advantage of the nonuniform ion distributions produced by thick electric double layers (EDLs) in nanochannels with heterogeneous surface charge. Specifically, we apply a voltage bias to gate electrodes embedded within the channel walls, tuning the surface charge in a region of the channel and subsequently altering the ionic strength and charge density in that region relative to the rest of the channel. The resulting nonuniform electromigration fluxes in the different regions serve to stack charged sample ions near an interface where a step change in zeta potential occurs, providing enhancement ratios superior to those exhibited in traditional microchannel field amplified sample stacking (FASS). Numerical simulations are performed to demonstrate the phenomenon, and resulting velocity and salt concentration profiles show good agreement with analytical results.

Keywords: nanofluidics, electrokinetic preconcentration, electroosmosis, electrophoresis

1. Introduction

Recent advances in micro- and nanoscale fabrication technologies have spurred the development of myriad novel devices for bioassays, DNA separation/amplification, and other lab-on-chip processes [1-6]. However, the small size scale of these devices introduces several obstacles that must be overcome through engineering prowess. A primary concern remains the necessity for sample analyte preconcentration in bioanalytical micro and nanofluidic devices [7,8]. Many innovative focusing techniques utilizing electrokinetic phenomena such as FASS, ion concentration polarization, isotachophoresis, isoelectric focusing, and concentration gradient focusing have been introduced in previous works to address and attempt to resolve this prevalent issue in on-chip applications [1-11]. Devices employing these mechanisms often exploit the competition between electroosmotic flow (EOF) and electrophoresis in micro- and nanofluidic systems in order to create regions of localized ion enrichment. These enriched ions can then be used for further downstream processing once the level of sample molecules reaches the threshold limit detectable by modern sensing capabilities.

Traditional microfluidic FASS involves the injection of a low concentration sample plug solution into a channel in order to create a conductivity gradient between the plug and the bulk fluid. These conductivity gradients produce electric field gradients which drive sample ions to "stack" at an equilibrium position where the various forces balance. Bharadwaj and Santiago comprehensively summarized the driving forces behind the stacking mechanism in microchannels [8], while Sustarich *et al* presented new findings of increased sample enhancement in the nanoscale regime due to pressure gradient induced flow focusing and electrostatic repulsion from finite-sized electric double layers (EDLs) relative to the channel height [9].

We extend these works by investigating the effects of thick, overlapped EDLs on the behavior of background electrolyte ions and sample ions in a nanochannel with nonuniform EOF. Other authors have previously investigated the effects of nonuniform EOF realized through means ranging from field effect control to EOF suppressing surface treatments [12-14]. Such channels have been shown to exhibit tremendous promise when it comes to controlling the behavior of bulk fluid and individual ions in applications such as nanofluidic diodes and field effect transistors [15-17].

Further, we have found that it is theoretically possible to create regions of nonuniform conductivity and electric fields within a single buffer solution by simply tailoring the surface charge in select regions of a nanochannel. We have therefore designed a tunable nanofluidic preconcentration system with embedded gate electrodes, allowing for field effect control of

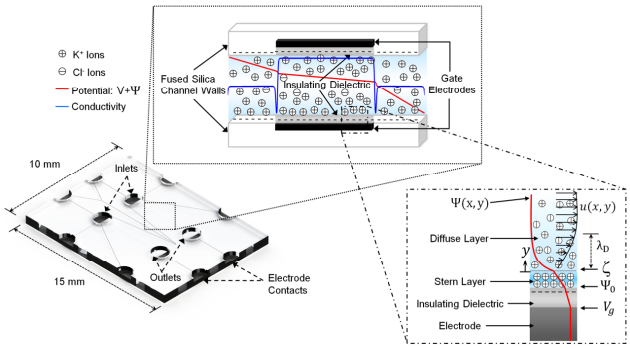

Figure 1: Diagram of the device with embedded electrodes (bottom left), with insets showing example ion distributions in the channel with a slightly modified surface charge (top center) and the EDL potential and velocity profiles near an embedded electrode (bottom right).

surface charge heterogeneity on the top and bottom channel walls with the application of a gate voltage (see Figure 1). This is used to generate nonuniform EOF and regions of controllable electrophoretic sample motion within the channel. Our technique is demonstrated with 2D numerical simulations using COMSOL Multiphysics finite element software. The numerical velocity, potential, and ion distributions in fully developed regions of the flow compare favorably with results from 1D analytical models for both thick and thin EDL cases. The particular mechanisms which cause sample enhancement are shown to only occur in channels with sufficiently large electric double layers relative to the channel height, and in channels with nonuniform surface charge. Sample enhancement ratios from our 2D simulations exceed those from traditional FASS. The unique characteristics of the ion-EDL interactions in nanochannels with nonuniform, thick EDLs suggest that there is room for further investigation and optimization of this process.

2. Theory

2.1 Electric Double Layer

When aqueous electrolyte solutions come into contact with a solid surface, various chemical interactions often leave the surface with a net charge. Free ions in solution are subsequently attracted to the charged surface, forming an electric double layer of ions. In the first layer adjacent to the wall, often referred to as the Stern Layer, a thin layer of oppositely charged counter-ions are electrostatically attracted to the charged surface so strongly that they are essentially adsorbed on the surface. Slightly farther away from the wall is a second layer of counter-ions that are still attracted to the surface but are free to move due to diffusive effects. Outside this diffuse layer, the ions in the bulk solution are shielded from the charged surface by the presence of the ions in the EDL. When an external electric field is applied, the ions within the EDL will migrate along field lines. The resulting shear stress from the motion of the fluid within the EDL pulls the bulk fluid along with it, generating an electroosmotic flow profile.

The resulting distribution of ions in the EDL near the charged surface gives rise to an electric potential profile which is largest in magnitude at the wall zeta potential ζ and decays to zero in the bulk fluid for large channels. This transverse potential distribution Ψ in the EDL can be related to the spatial free charge density of ions in solution using Poisson's equation,

$$-\varepsilon_0 \varepsilon_\mathrm{f} \nabla^2 \Psi = \rho_\mathrm{E}, \tag{1}$$

where ε_0 is the permittivity of free space, ε_f is the relative permittivity of the electrolyte solution, and ρ_E is the local volumetric charge density. The charge density effectively represents the net charge present due to a local imbalance of cations and anions in solution, which for a binary monovalent electrolyte such as KCl can be expressed as $\rho_\mathrm{E} = F(c_+ - c_-)$, where F is Faraday's constant, c_+ is the molar concentration of cations, and c_- is the molar concentration of anions. Using Boltzmann statistics to account for the relative energy content of the ions in solution, the distribution of ions near a charged surface is approximated as an exponentially decaying function

$$c_\mathrm{i} = c_{\mathrm{i},\infty} \exp\left(-\frac{z_\mathrm{i} e_0 \Psi}{k_\mathrm{b} T}\right), \tag{2}$$

where z_i is the ion valence, e_0 is the elementary charge, $k_b T$ represents the thermal energy, and $c_{i,\infty}$ is the bulk concentration of cations and anions sufficiently far from the surface. The characteristic length scale over which the potential and ion distributions decay within the EDL is referred to as the Debye length, which for a symmetric, monovalent electrolyte can be expressed as

$$\lambda_D = \sqrt{\frac{\varepsilon_0 \varepsilon_f k_b T}{2 c_\infty {e_0}^2}}. \quad (3)$$

For low concentration electrolytes ($c_\infty < 1$ mM) in nanochannels, this characteristic length can approach and even exceed the height of the channel. In such situations, it is no longer appropriate to assume that the ion concentrations far away from the channel walls (i.e. along the channel center) are the same as those in the bulk fluid within the reservoirs supplying the channel. The centerline concentration in the channel is instead determined by the potential Ψ_c at the centerline, and the Boltzmann distribution modifies to

$$c_i = c_\infty \exp\left(-\frac{e_0 z_i \Psi_c}{k_b T}\right) \exp\left(-\frac{e_0 z_i (\Psi - \Psi_c)}{k_b T}\right). \quad (4)$$

Using the definition $\rho_E = F(c_+ - c_-)$ and assuming a 1D potential profile, we use the method presented by Baldessari to integrate Poisson's equation and find a resulting potential profile in the different regions of the channel [18]. It should be noted here that for channels with modified zeta potentials in the middle region (see Figure 2), the "bulk" concentration c_∞ of ions in this region will not necessarily be equal to the supplying inlet or outlet reservoir concentrations, and must be solved as an additional unknown using channel-to-well equilibrium via a species conservation equation. If the surface charge is known instead of the zeta potential in a given region of the channel, the two can be related through the potential gradient at the wall through the relation

$$\sigma_w = -\varepsilon_0 \varepsilon_f \left.\frac{d\Psi}{dy}\right|_{y=0}. \quad (5)$$

2.2 Velocity and Electric Fields

The inherently low Reynolds number associated with flows in nanofluidic devices allows us to use the incompressible forms of the Stokes equation and the continuity equation to describe the conservation of momentum within a nanochannel for a fluid experiencing an electric body force,

$$0 = \mu \nabla^2 \mathbf{u} - \nabla P + \rho_E \mathbf{E}; \qquad \nabla \cdot \mathbf{u} = 0, \quad (6)$$

where P is the pressure within the fluid, μ is the dynamic viscosity of the fluid, $\mathbf{u}$ is the velocity field, and $\mathbf{E}$ is the externally applied electric field. Substituting the charge density from Poisson's equation into the electric body force term in (6) and assuming a 1D fully developed flow, we obtain the following equation

$$0 = \mu \frac{\partial^2 u}{\partial y^2} - \frac{\partial P}{\partial x} - \varepsilon_0 \varepsilon_f E_x \frac{\partial^2 \Psi}{\partial y^2}. \quad (7)$$

This equation can be directly integrated with a midplane symmetry condition and a no slip condition at the wall, resulting in the traditional 1D EOF profile

$$u(y) = \frac{-1}{2\mu}\frac{dP}{dx}(y^2 - Hy) - \frac{\varepsilon E_x \zeta}{\mu}\left(1 - \frac{\Psi(y)}{\zeta}\right). \quad (8)$$

We use the 1D model of Sustarich *et al* to find the internal pressure gradients, electric fields, and resulting flow profiles in the various regions. This model applies continuity and a known pressure drop along the channel to solve for the internal pressure gradients in terms of the electric fields. The electric fields are then solved with the constraint that the area averaged electrolyte ion fluxes due to convection and electromigration must remain constant throughout the channel

$$\overline{uc_i} + b_i \bar{c}_i E = const., \quad (9)$$

where $b_i = \frac{z_i e_0 D_i}{k_b T}$ [7]. These equations are solved for the unknown electric fields and the unknown "bulk" concentration c_∞ of ions in the modified region. The resulting potential and BGE ion profiles are then found from the method described in [18], and the velocity profiles are calculated from (8).

3. 2D Numerical Model

Commercial finite element simulation software such as COMSOL Multiphysics has been used extensively in previous works to numerically model electrokinetic flows in micro- and nanofluidics [1,4,7,10,19]. In this paper, we

use COMSOL v5.1 to simulate a 2D model of electroosmotically driven flow and the electrophoretic stacking of sample ions in a nanochannel with a modified zeta potential in the middle 50% of the channel. The governing equations are similar to the equations presented in sections 2.1 and 2.2; however, we use the more highly coupled Poisson-Nernst-Planck system of equations to account for the effect of the local ion distributions on the EDL potential. As such, we don't explicitly assume a Boltzmann distribution of ions in our simulation. Instead, we simply represent the spatial free charge density ρ_E as a local imbalance of cations and anions in solution, the concentrations of which are governed by the Nernst-Planck equation for a species experiencing convection, diffusion, and electromigration. Poisson's equation for the EDL transverse potential distribution then becomes

$$-\varepsilon_0\varepsilon_f\nabla^2\Psi = F(c_+ - c_-), \tag{10}$$

and the Nernst-Planck equation is given by

$$\frac{\partial c_i}{\partial t} + \mathbf{u}\cdot\nabla c_i = D_i\nabla\cdot\left(\nabla c_i + \frac{e_0 z_i c_i \nabla(V+\Psi)}{k_b T}\right). \tag{11}$$

We model (10) using a "Coefficient Form PDE" module, and (11) for the various ionic species using the "Transport of Diluted Species" module within COMSOL. The convection term in (11) is due to the advective transport of ions from the electroosmotic flow, and is coupled to the Stokes equation and mass continuity

$$\begin{cases} 0 = \mu\nabla^2\mathbf{u} - \nabla P + F(c_+ - c_-)\mathbf{E} \\ \nabla\cdot\mathbf{u} = 0. \end{cases} \tag{12}$$

This electroosmotic flow field is modeled in COMSOL using the "Creeping Flow" module. Finally, Ohm's Law and current continuity are modeled with the "Electric Currents" module to describe the electric field within the fluid

$$\begin{cases} \mathbf{J} = \sigma_E\mathbf{E}; & \mathbf{E} = -\nabla V \\ \nabla\cdot\mathbf{J} = 0, \end{cases} \tag{13}$$

where $\mathbf{J}$ is the local current density, σ_E is the electrical conductivity, and V is the externally applied potential. The electrical conductivity depends on the local number of charge carriers, and contains components related to the convective and conductive currents in the channel [18]. The conductivity can be written in terms of the local background ion concentrations as

$$\sigma_E = \frac{u_x F(c_+ - c_-)}{E_x} + \frac{e_0}{k_b T}F(c_+ + c_-)\overline{D}. \tag{14}$$

The first term in (14) represents the current due to a nonzero charge being advected downstream by the EOF, while the second term represents the current generated by the electromigration of individual background electrolyte (BGE) ions in the presence of the external field. For thin EDLs,

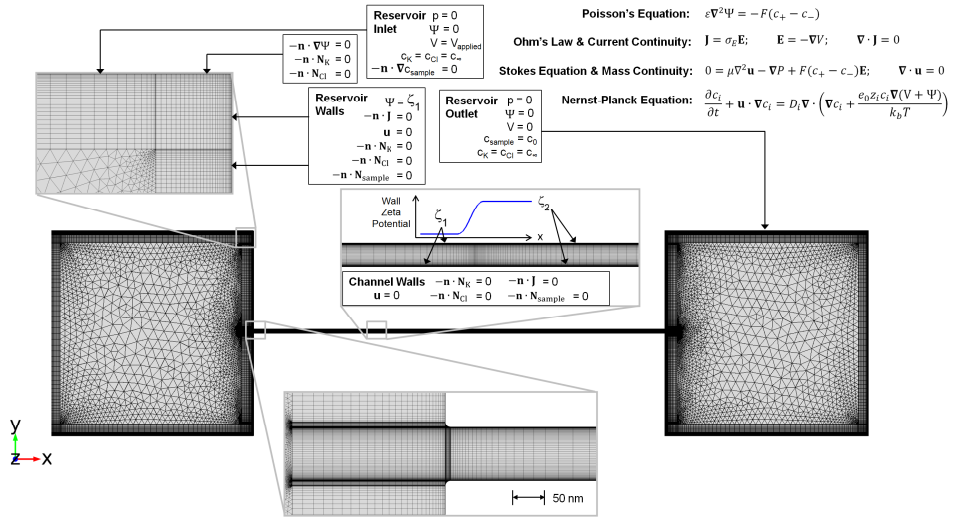

Figure 2: Diagram of the numerical mesh and boundary conditions used in the COMSOL simulations. Approximately 340,000 mesh elements were used in the various regions to properly resolve the electric double layers, ion transport, and electroosmotic flow within the channel and reservoirs.

most of the fluid remains electrically neutral where $c_+ = c_-$, and the first term is negligible compared to the second. However, we are investigating nanochannels with electrolyte concentrations sufficiently low to cause significant overlapping of the EDLs, so the contribution of the local charge density to the electrical conductivity cannot be neglected [19].

A finite element mesh of approximately 340,000 distributed mapped elements and triangular elements was employed throughout the channel and reservoirs. This custom mesh was used to ensure proper resolution of fine gradients within the EDLs and near transition regions while still allowing for computations that were both time and memory efficient. Figure 2 depicts a diagram of the 2D model with the mesh and boundary conditions for the nanochannel and supplying reservoirs. The electrolyte used in all simulations was KCl, with $D_K = 1.96 \times 10^{-9}$ m^2/s and $D_{Cl} = 2.03 \times 10^{-9}$ m^2/s. The sample diffusivity was fixed at $D_s = 1 \times 10^{-9}$ m^2/s and, unless otherwise noted, the sample charge was fixed at z = -2.

4. Results

In order to verify that our numerical model produces reasonable results, we first compare the 2D and 1D models for a relatively simple case of non-overlapping EDLs. We simulated a 0.5 mm long, 100 nm tall channel filled with a solution of 2.5mM KCl, corresponding to a Debye length of about $\lambda_D = 6.1$ nm. An externally applied potential of 5 V was used to drive the simulated EOF with a nominal electric field of 10,000 V/m. The unmodified and modified zeta potentials were -25 mV and -5 mV, respectively.

Figure 3 shows a comparison of the resulting vertical profiles of the EDL potential, BGE salt concentration, and axial velocity. A plot of the centerline BGE salt concentration based on a 1D axial transport equation from [7] is also included. The profiles demonstrate excellent agreement between the simulated and analytical results, with perhaps the slight exception of the centerline profile near the zeta potential transitions. This is to be expected, however, as the 1D analytical model cannot account for localized 2D effects such as flow focusing and dispersion near the transitions.

We validated our model further for a case with thick electric double layers, comparing various profiles with the 1D analytical model as the zeta potential in the middle of the channel was varied in a 0.01mM solution. The results show excellent agreement for the potential and charge density profiles, although the velocity profiles seem to increasingly deviate for the more uniform cases. This is likely due to the fact that the analytical results assumed zero pressure difference between channel inlet and outlet, whereas in the simulation and in experimental situations the effect of the fluid accelerating and decelerating in the respective reservoirs would cause an adverse pressure gradient across the channel and slow the fluid slightly. This effect would become more prominent for thicker EDL cases due to the nonzero electric body force everywhere, as well as for faster-moving flows; hence the higher deviation for the more uniform cases.

Our simulation results in Figure 4 also show that the sample stacking only occurs when the nonuniformities in velocity, potential, and ion distributions throughout the channel are

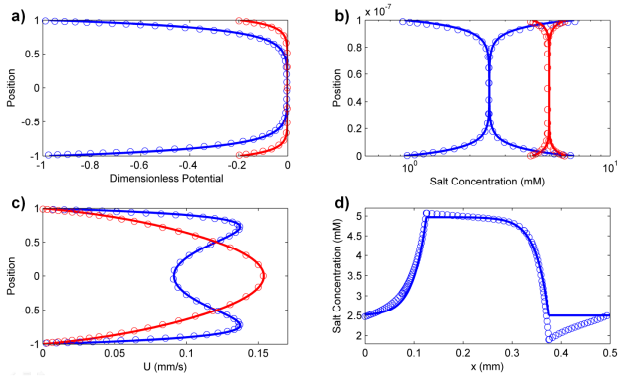

Figure 3: Comparison of thin EDL analytical (solid lines) vs. simulation results (open circles). The profiles show excellent agreement for (a) the transverse potential, (b) BGE ion, and (c) velocity profiles in both region 1 (blue) and region 2 (red). Discrepancies in (d) the centerline BGE ion profile are likely due to 2D effects such as dispersion.

sufficiently large. This requires thick electric double layers, such that the background ion distributions and resulting electromigrative fluxes are modified sufficiently near the centerline. For thin electric double layers, the electrostatic interactions of the EDL are confined near the wall and a majority of the fluid is at the bulk concentration and bulk conductivity, which leads to uniform electric fields and sample fluxes. Additionally, a channel with uniform wall potential and conductivity distributions will have a uniform electrochemical potential and not allow for any local ion enrichment or depletion along the length of the channel. A nonuniform surface potential distribution and thick EDLs are thus essential to induce the heterogeneity required within the single buffer solution to produce the gradients that lead to stacking. Highly charged sample ions are more strongly affected by these field gradients and can be effectively concentrated to higher levels.

Figure 5 depicts the temporal evolution of a 2D sample concentration profile within the channel, showing how a negatively charged sample stacks near an interface where a smooth step change in zeta potential occurs. Due to the thick electric double layers, the sample is repelled towards the center of the channel, increasing the local enhancement along the centerline. The intrinsic EDL potential Ψ along the centerline is nonzero due to the thick EDLs, so there is an additional axial potential gradient along the channel as the flow transitions from one region to the next. This additional potential gradient can be larger in magnitude than the axial gradient in the applied potential, and the net electric field can change direction locally as a result. This enhances the stacking and creates an electrophoretic trapping region, as shown in Figure 5. Once the sample starts to accumulate, diffusion becomes a significant driving factor in the transport of the sample through the channel. The diffusive flux eventually balances the electromigrative flux and the convective flux in the enhancement region as the system reaches a steady state. Near the other zeta potential transition, the opposite effect occurs as the EDL potential gradient is in the same direction as the external field. Sample ions here are further accelerated, creating a localized depletion region.

5. Conclusions

In this work, we used COMSOL Multiphysics to model the 2D electroosmotic flow of a dilute background electrolyte and the electrophoretic stacking of sample ions in a nanochannel with selectively modified surface charge. We showed that these particular stacking and focusing effects only occur in channels with sufficiently large step changes in zeta potential, and for cases in which the EDLs are sufficiently large relative to the channel height. Our approach can potentially achieve several hundred-fold sample enhancement ratios, notably higher than those limited by conductivity ratios in conventional FASS[7,8]. Resulting velocity field, potential, and ion distributions were

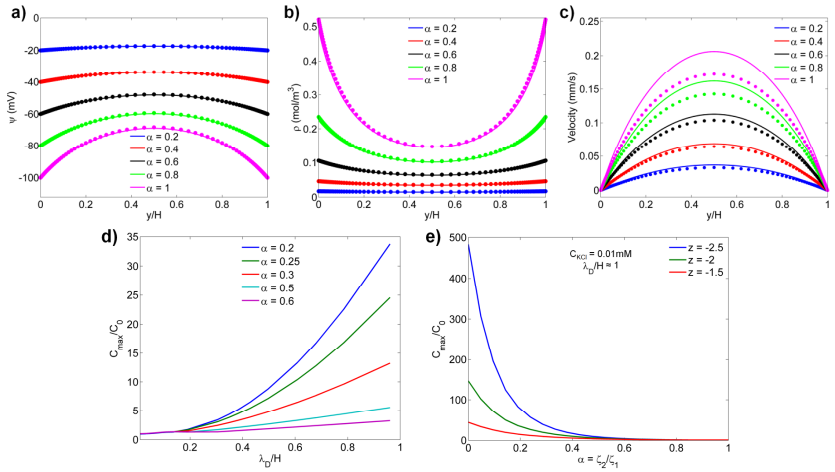

Figure 4: Simulation results for thick EDLs. Analytical (solid lines) vs. simulation (solid circles) results are shown for (a) the potential, (b) the charge density, and (c) the velocity profiles for varying zeta potentials in region 2. Sample enhancement ratios are shown in (d) for varying zeta potential ratios and EDL thicknesses, and in (e) for varying zeta potential and sample charge. The zeta potential in region 1 was fixed at -100 mV for these simulations.

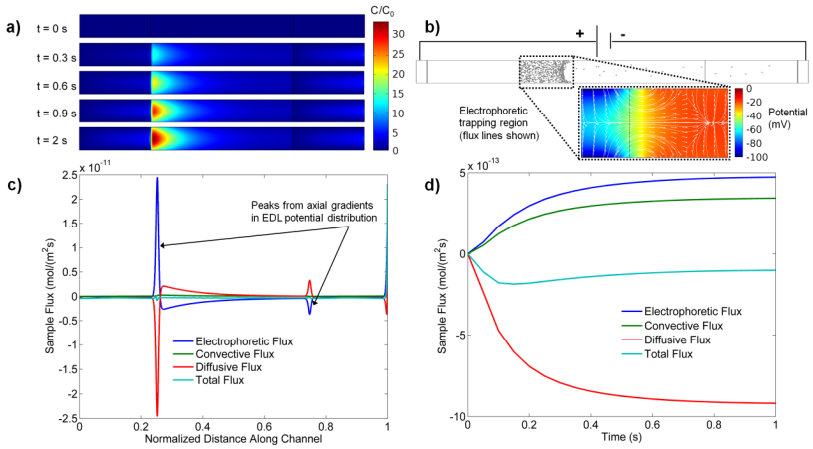

Figure 5: (a) Transient evolution of 2D sample concentration profile within the channel, (b) a diagram depicting electrophoretic trapping of particles in a simulation, (c) steady state fluxes along the channel centerline, and (d) area averaged time-dependent sample fluxes at the location of maximum enhancement. The effect of the axial EDL potential gradient is visible in the positive electrophoretic flux of the negative sample in (d), the peaks near the transition locations in (c), and flux lines near the electrophoretic trap in (b).

validated through comparison with existing analytical techniques to solve the 1D Poisson-Boltzmann equation, Stokes equation, and Nernst-Planck equation [7,18].

These results provide encouraging indications that it is possible to perform stationary field-amplified sample preconcentration in nanochannels without using multiple electrolyte solutions, but by simply inducing electric field gradients through the tailoring of wall surface charge uniformity via embedded electrodes. The resulting enhancement in our simulations can exceed that of traditional microchannel-based stacking mechanisms and rivals that of similar nanoscale methods [1,2,7-11], revealing another promising technique for sample preconcentration in nanofluidic devices.

6. References

1. Yu M, Hou Y, Zhou H, and Yao S, An on-demand nanofluidic concentrator *Lab on Chip* **15**, 1524-32 (2015)
2. Hsu W, Harvie D J, Davidson M R, Jeong H, Goldys E M, and Inglis D W, Concentration gradient focusing and separation in a silica nanofluidic channel with a non-uniform electroosmotic flow *Lab on Chip* **14**, 3539-49 (2014)
3. Stein D, Deurvorst Z, van der Heyden F H J, Koopmans W J A, Gabel A, and Dekker C, Electrokinetic Concentration of DNA Polymers in Nanofluidic Channels *Nano Letters* **10**, 765-72 (2010)
4. Napoli M, Eijkel J C T, and Pennathur S, Nanofluidic technology for biomolecule applications, a critical review *Lab on Chip* **10**, 957-85 (2010)
5. Kim S J, Song Y, and Han J, Nanofluidic concentration devices for biomolecules utilizing ion concentration polarization: theory, fabrication, and applications *Chem. Soc. Rev.* **39**, 912-22 (2010)
6. Sparreboom W, van den Berg A, Eijkel J C T, Principles and applications of nanofluidic transport, *Nature Nanotechnology*, **4**, 713-20 (2009)
7. Sustarich J, Storey B, and Pennathur S, Field-amplified sample stacking and focusing in nanofluidic channels *Phys Fluids* **22**, 112003 (2010)
8. Bharadwaj R and Santiago J G, Dynamics of field-amplified sample stacking *J. Fluid Mech.* **543**, 57-92 (2005)
9. Hsu W, Inglis D W, Startsev M A, Goldys E M, M Davidson M R, Harvie D J, Isoelectric Focusing in a Silica Nanofluidic Channel: Effects of Electromigration and Electroosmosis, *Anal. Chem.,* **86**, 8711-18 (2014)
10. Plecis A, Nanteuil C, Haghiri-Gosnet A, Chen Y, Electropreconcentration with Charge-Selective Nanochannels, *Anal. Chem.,* **80**, 9542-50 (2008)
11. Quist J, Janssen K G H, Vulto P, Hankemeier T, van der Linden H J, Single-Electrolyte Isotachophoresis Using a Nanochannel-Induced Depletion Zone, *Anal. Chem.*, **83**, 7910-15 (2011)
12. Herr A E, Molho J I, Santiago J G, Mungal M G, Kenny T W, Electroosmotic Capillary Flow with Nonuniform Zeta Potential, *Anal. Chem.,* **72**, 1053-57 (2000)
13. Bhattacharyya S, Nayak A K, Electroosmotic flow in micro/nanochannels with surface potential heterogeneity: An analysis through the Nernst-Planck

model with convection effect, *Colloids and Surfaces A: Physicochem. Eng. Aspects*, **339**, 167-77 (2009)
14. Hughes C, Yeh L, Qian S, Field Effect Modulation of Surface Charge Property And Electroosmotic Flow in a Nanochannel: Stern Layer Effect, *J. Phys. Chem.,* **117**, 9322-31 (2013)
15. Daiguji H, Ion transport in nanofluidic channels, *Chem. Soc. Rev.,* **39**, 901-11 (2010)
16. Cheng L, Guo L J, Nanofluidic diodes, *Chem. Soc. Rev.,* **39**, 923-38 (2010)
17. Guan W, Li S X, Reed M A, Voltage gated ion and molecule transport in engineered nanochannels: theory, fabrication and applications, *Nanotechnology,* **25**, 122001 (2014)
18. Baldessari F, Electrokinetics in nanochannels Part I. Electric double layer overlap and channel-to-well-equilibrium, *J. Colloid and Interface Science*, **325**(2) , 526-38 (2008)
19. McCallum C, Pennathur S, Accounting for electric double layer and pressure gradient-induced dispersion effects in microfluidic current monitoring, *Microfluid Nanofluid*, 20:13 (2016)

7. Acknowledgements

We greatly acknowledge our funding sources, the Institute for Collaborative Biotechnologies through grant W911NF-09-001 from the U.S. Army Research Office, and grant DAAD19-03-D-0004 from the U.S. Army Research Office.